Scuola di Dottorato Leonardo da Vinci – a.a. 2008/09

LASER: CARATTERISTICHE, PRINCIPI FISICI, APPLICAZIONI

Versione 2 – Luglio 09 – http://www.df.unipi.it/~fuso/dida

Parte 7
Proprietà della luce laser, emissione impulsata ed impulsi ultra-brevi

Lu 27.07.09 15-17 aula DIC

SOMMARIO

Sappiamo che la luce laser ha proprietà uniche (monocromaticità, coerenza, brillanza, etc.) e sappiamo come è fatto un laser

- Proprietà della luce laser e strategie di miglioramento:
  - monocromaticità
  - coerenza temporale e spaziale
  - brillanza

- Laser ad alta ed altissima intensità con impulsi brevi e ultra-brevi:
  - Q-switching
  - mode locking ed impulsi ultra-brevi

Obiettivo : capire l'origine delle proprietà del laser

Obiettivo secondario: discutere alcune strategie per ottimizzare l'operazione laser ed ottenere risultati specifici

MONOCROMATICITÀ

1.4. PROPERTIES OF LASER BEAMS

Laser radiation is characterized by an extremely high degree of monochromaticity, coherence, directionality, and brightness. We can add a fifth property, viz., short duration, which refers to the capability of producing very short light pulses, a less fundamental but nevertheless very important property. We now consider these properties in some detail.

1.4.1. Monochromaticity

This property is due to the following two circumstances: (1) Only an em wave of frequency ν given by Eq. (1.1.1) can be amplified. (2) Since a two-mirror arrangement forms a resonant cavity, oscillation can occur only at the resonance frequencies of this cavity. The latter circumstance leads to an often much narrower laser linewidth (by as much as 10 orders of magnitude) than the usual linewidth of the transition $2 \rightarrow 1$, as observed in spontaneous emission.

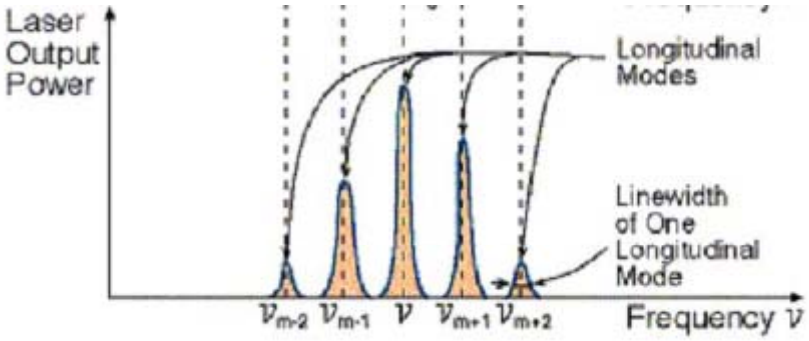

Larghezza di riga del laser regolata da larghezza di riga della cavità

Il carattere monocromatico dipende da:
- Selezione singolo modo longitudinale;
- Larghezza del modo (cavità);
- (spesso) selezione modo trasversale

Avevamo definito: $Q = 2\pi c/(\alpha\lambda) = \omega/\alpha = \omega\tau$
τ: vita media fotone in cavità

Andamento temporale campo e.m. nella cavità: $E(t) = E_0 e^{-i\omega t} e^{-\alpha t}$

Componente Fourier a pulsazione Ω:

$$\tilde{E}(\Omega) \sim \int_0^\infty E(t) e^{i\Omega t} dt = E_0 \int_0^\infty e^{i(\Omega - \omega + i\alpha)t} dt \sim$$

$$\sim \frac{E_0}{i\left[(\Omega - \omega) + i\alpha\right]}$$

Densità energia e.m. (ovvero potenza):

$$u(\Omega) \sim |\tilde{E}(\Omega)|^2 = \frac{|E_0|^2}{\left[(\Omega - \omega)^2 + \alpha^2\right]}$$

Larghezza di riga della cavità: $\Delta\omega_{cavità} \sim \alpha = \frac{\omega}{Q}$

STRATEGIE DI AUMENTO *Q*

Intracavity etalon

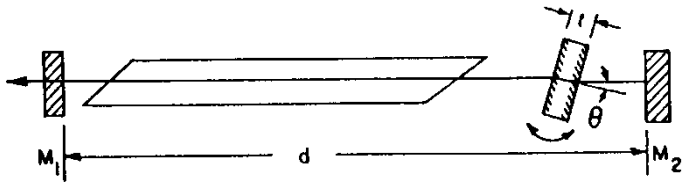

Fig.5.36. Single-mode operation by inserting a tilted etalon inside the laser resonator

In optics, a **Fabry-Pérot interferometer** or **etalon** is typically made of a transparent plate with two reflecting surfaces, or two parallel highly reflecting mirrors. (Technically the former is an etalon and the latter is an interferometer, but the terminology is often used inconsistently.) Its transmission spectrum as a function of wavelength exhibits peaks of large transmission corresponding to resonances of the etalon. It is named after Charles Fabry and Alfred Perot.[1] "Etalon" is from the French *étalon*, meaning "measuring gauge" or "standard".[2]

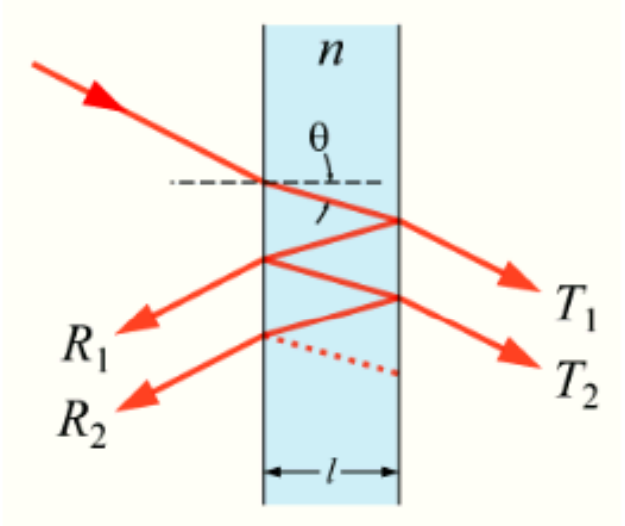

A Fabry-Pérot etalon. Light enters the etalon and undergoes multiple internal reflections.

The phase difference between each succeeding reflection is given by δ:

$$\delta = \left(\frac{2\pi}{\lambda}\right) 2nl\cos\theta.$$

f.s.r. etalon: $\delta = m\pi$

If both surfaces have a reflectance R, the transmittance function of the etalon is given by:

$$T_e = \frac{(1-R)^2}{1+R^2-2R\cos(\delta)} = \frac{1}{1+F\sin^2(\frac{\delta}{2})}$$

where $F = \frac{4R}{(1-R)^2}$ is the *coefficient of finesse*.

Finezza dell'etalon

The varying transmission function of an etalon is caused by interference between the multiple reflections of light between the two reflecting surfaces. Constructive interference occurs if the transmitted beams are in phase, and this corresponds to a high-transmission peak of the etalon. If the transmitted beams are out-of-phase, destructive interference occurs and this corresponds to a transmission minimum. Whether the multiply-reflected beams are in-phase or not depends on the wavelength (λ) of the light (in vacuum), the angle the light travels through the etalon (θ), the thickness of the etalon (l) and the refractive index of the material between the reflecting surfaces (n).

FINEZZA E LARGHEZZA DI RIGA

$$T_e = \frac{(1-R)^2}{1+R^2-2R\cos(\delta)} = \frac{1}{1+F\sin^2(\frac{\delta}{2})}$$

where $F = \frac{4R}{(1-R)^2}$ is the *coefficient of finesse*.

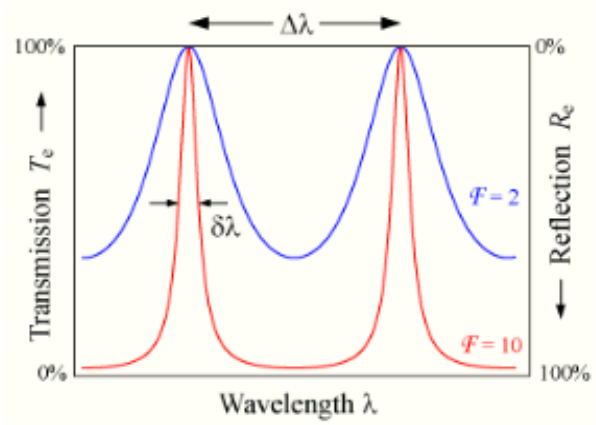

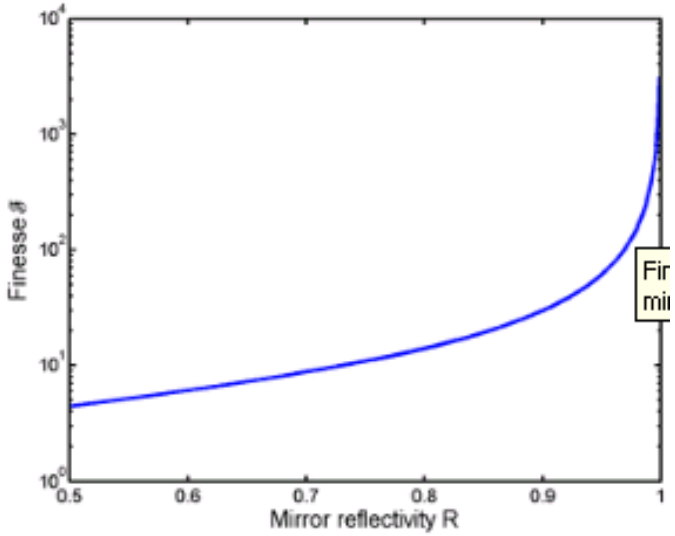

Possibile realizzare etalon con finezza > 10^3
(a scapito della trasmissione media, cioè
fuori dai modi consentiti)

Larghezze di riga *tipiche* per laser CW (in continua):

- Laser a gas (HeNe, Ar^+,…): $\Delta\nu < 1$ MHz (anche < 1 kHz per laser con cavità ultrastabili)
- Laser a stato solido (Nd:YAG, TiSa, centri di colore, …): $\Delta\nu \sim 1$ MHz (anche < 10 kHz con etalon)
- Laser a colorante: $\Delta\nu \sim 100$ MHz (fino a 100 kHz per laser con etalon)
- Laser a diodo: $\Delta\nu \sim 1$ MHz (anche < 10 kHz per laser con cavità esterna)

Attenzione: drift termico e jitter introducono fluttuazioni a tempi “lunghi”!

LIMITE QUANTISTICO

Schawlow–Townes Linewidth

Definition: linewidth of a single-frequency laser with quantum noise only

Even before the first laser was experimentally demonstrated, Schawlow and Townes calculated the fundamental (quantum) limit for the linewidth of a laser [1]. This lead to the famous *Schawlow–Townes equation*:

Esiste limite quantistico per larghezza di riga dovuto a fluttuazioni quantistiche (em. spont.)

$$\Delta\nu_{\text{laser}} = \frac{\pi h\nu \left(\Delta\nu_c\right)^2}{P_{\text{out}}}$$

Es.: HeNe, $h\nu$=2eV, $\Delta\nu_C$=1MHz, P_{out}=1mW → $\Delta\nu_{S.T.}$~1mHz!!

with the photon energy $h\nu$, the resonator bandwidth $\Delta\nu_c$ (full width at half-maximum, FWHM), and the output power P_{out}. It has been assumed that there are no parasitic cavity losses. (Compared with the original equation, a factor 4 has been removed because of a different definition of the resonator bandwidth.)

It is often claimed that the phase noise level corresponding to the Schawlow–Townes linewidth is a result of spontaneous emission into the laser mode. Although this picture is intuitive, it is not completely correct. Both the laser gain and the linear losses of the laser resonator contribute equal amounts of quantum noise to the intracavity light field. This means that even when replacing laser gain with some noiseless amplification process, the phase noise would only decrease to half of the Schawlow–Townes value [2].

Carefully constructed solid-state lasers can have very small linewidths in the region of a few kilohertz, which is still significantly above their Schawlow–Townes limit: technical excess noise makes it difficult to reach that limit. The linewidth of semiconductor lasers is also normally much larger than according to the original equation (without the α factor). This, however, is largely caused by amplitude-to-phase coupling effects (which can be quantified with the linewidth enhancement factor), and not by technical excess noise.

Altre fluttuazioni “tecnologiche” (es. fase/ampiezza) generalmente più importanti di limite Schawlow-Townes

SINTONIZZABILITÀ

Lo spettro di guadagno del mezzo attivo ha normalmente larghezze “piccole” (typ. 1-10GHz)
→Eventuale sintonizzabilità è selezione dei modi (oppure scelta della riga attiva, e.g. Ar^+,CO_2)

Eccezioni: laser con mezzi attivi “a banda larga”:
-Laser a colorante (in soluzione o allo stato solido
-Laser a diodo (bande invece di livelli discreti…)

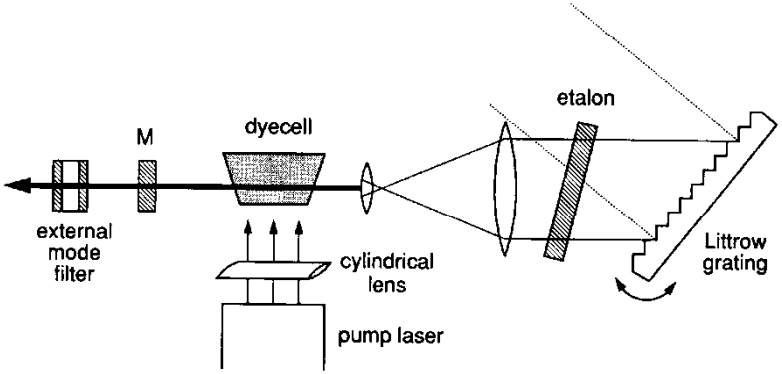

Fig.5.44. Short Hänsch-type dye-laser cavity with Littrow grating and mode selection either with an internal etalon or an external FPI as "mode filter" [5.57]

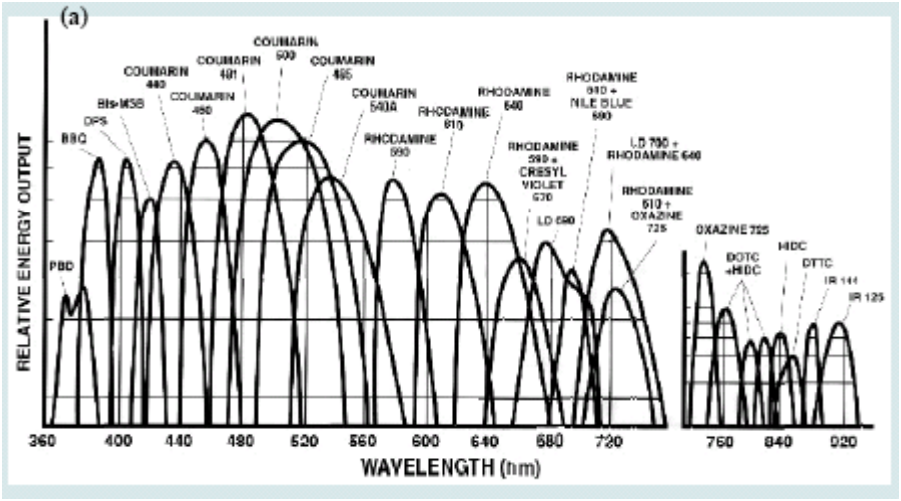

Cavità terminate da reticolo di diffrazione invece che specchi

When there is a need to separate light of different wavelengths with high resolution, then a diffraction grating is most often the tool of choice. This "super prism" aspect of the diffraction grating leads to application for measuring atomic spectra in both laboratory instruments and telescopes. A large number of parallel, closely spaced slits constitutes a diffraction grating. The condition for maximum intensity is the same as that for the double slit or multiple slits, but with a large number of slits the intensity maximum is very sharp and narrow, providing the high resolution for spectroscopic applications. The peak intensities are also much higher for the grating than for the double slit.

DIFFRACTION GRATINGS

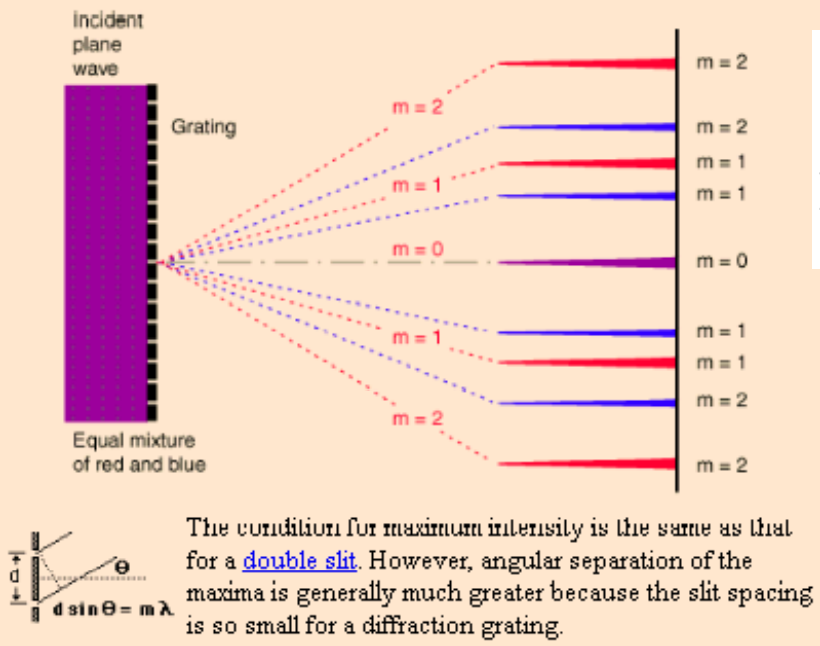

The condition for maximum intensity is the same as that for a double slit. However, angular separation of the maxima is generally much greater because the slit spacing is so small for a diffraction grating.

$$d \sin\theta_m = m\lambda.$$

Tipicamente d = *1/3600-1/600* mm^{-1}

It is straightforward to show that if a plane wave is incident at an angle θ_i, the grating equation becomes

$$d\,(\sin\theta_m + \sin\theta_i) = m\lambda.$$

The light that corresponds to direct transmission (or specular reflection in the case of a reflection grating) is called the zero order, and is denoted $m = 0$. The other maxima occur at angles which are represented by non-zero integers m. Note that m can be positive or negative, resulting in diffracted orders on both sides of the zero order beam.

La diffrazione dal reticolo segue le leggi dell'interferenza da sorgenti (slits) multiple

Riflessione massima ad una determinata combinazione di angoli di incidenza e riflessione

La cavità terminata da un reticolo ha perdite dipendenti dalla lunghezza d'onda

↓

Laser può operare solo se le perdite sono minori del guadagno

↓

Emissione sintonizzabile

STABILIZZAZIONE LASER

Laser possono essere stabilizzati rispetto a vari parametri (e.g., ampiezza, frequenza)

Strategia di stabilizzazione: feedback elettronico (PID) su riferimento → lunghezza cavità

- The optical frequency of a single-frequency laser, or the frequency of one line of the frequency comb from a mode-locked laser, can be stabilized via resonator length control. The feedback signal can be obtained e.g. by recording a beat note with a second laser, by measuring the transmission or reflection of a very stable reference cavity, or by measuring the transmission of some absorption cell (e.g. an iodine cell), possibly using Doppler-free spectroscopy. A frequently used technique for generating an error signal is the Pound-Drever-Hall method [2, 3], using a weak phase modulation of the light which is sent to a reference cavity. A scheme not requiring such modulation is the Hänsch-Couillaud method [1].

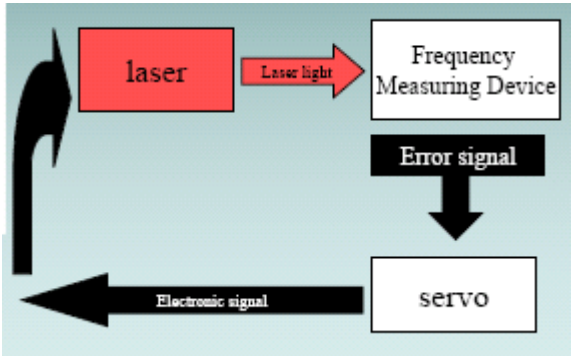

Cella di riferimento (assorbitore)

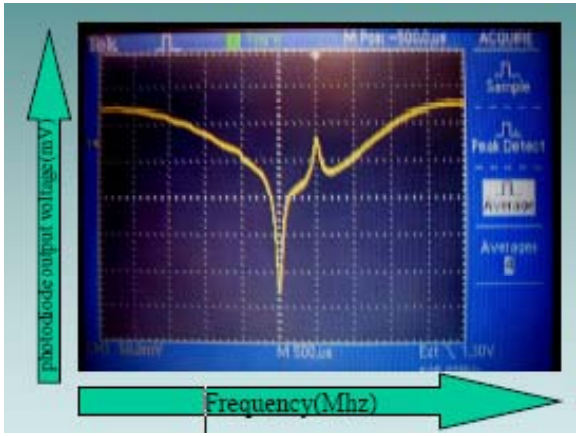

Frequency modulation : the wavelength of the laser is scanned across the atomic transition, and the wavelength modulation is seen as varying amplitude modulation.

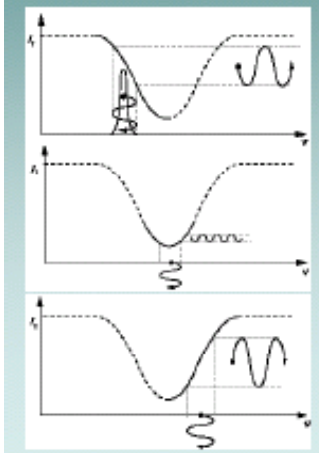

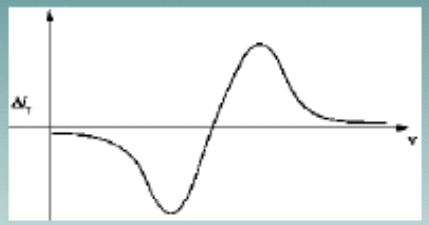

- The ratio of AM to FM versus the laser frequency results in this derivative signal
- This signal is at zero when the laser is on resonance
- Use this as the error signal for peak locking the laser

Tecniche di stabilizzazione più raffinate (e.g., Pound-Drever) per arrivare a stabilità 10^{-10} - 10^{-12} e larghezze di riga < 1Hz (su tempi brevi)

PROPRIETÀ LUCE LASER

Già annunciate:
- *Monocromaticità*
- Coerenza (spaziale e temporale)

Non ancora introdotte:
- [Brillanza (intensità e collimazione/focalizzazione)]

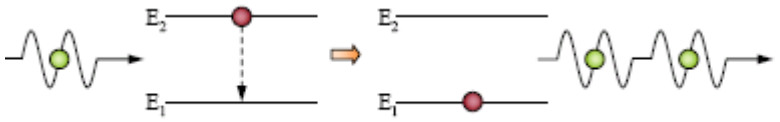

EMISSIONE COERENTE

DUE FOTONI INDISTINGUIBILI: STESSA FREQUENZA, DIREZIONE, FASE E POLARIZZAZIONE

In termini semplici possiamo pensare ad una sorta di "ordine" dei fotoni

In pratica una coerenza elevata implica una elevata focalizzabilità del laser (macchia focale molto piccola, intensità elevata)

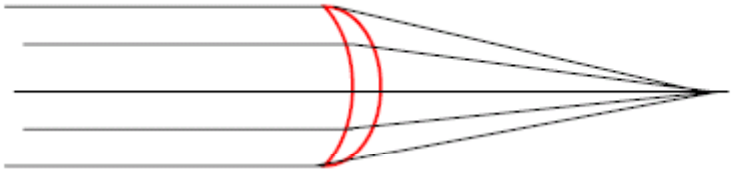

COERENZA I

Coerenza nasce da emissione stimolata (e, in genere, proveniente da piccolo volume di mezzo attivo)
Come si può caratterizzare meglio?

Definizioni di coerenza temporale e spaziale

The radiation emitted by an extended source S generates a total field amplitude A at the point P which is a superposition of an infinite number of partial waves with the amplitudes A_n and the phases ϕ_n emitted from the different surface elements dS (Fig.2.21), i.e.,

$$A(P) = \sum A_n(P)\, e^{i\phi n(P)} = \sum [A_n(0)/r_n^2]\, e^{i(\phi n_0 + 2\pi r_n/\lambda)} , \qquad (2.89)$$

where $\phi_{n0}(t) = \omega t + \phi_n(0)$ is the phase of the n^{th} partial wave at the surface element dS of the source. The phases $\phi_n(r_n,t)$ depend on the distances r_n from the source and on the angular frequency ω.

If the phase differences $\Delta\phi_n = \phi_n(P,t_1) - \phi_n(P,t_2)$ at a *given point* P between two different times t_1, t_2 are nearly the same for all partial waves, the radiation field at P is called *temporally coherent*. The maximum time intervall $\Delta t = t_2 - t_1$ for which $\Delta\phi_n$ for all partial waves differ by less than π is termed the *coherence time* of the radiation source. The path length $\Delta s_c = c\Delta t$ travelled by the wave during the coherence time Δt is the *coherence length*.

If a constant time-independent phase difference $\Delta\phi = \phi(P_1) - \phi(P_2)$ exists for the total amplitudes $A = A_0 e^{i\phi}$ at two different points P_1, P_2, the radiation field is called *spatially coherent*. All points P_m, P_n which fulfil the condition that for all times t, $|\phi(P_m,t) - \phi(P_n,t)| < \pi$, have nearly the same optical path difference from the source. They form the *coherence volume*.

The superposition of coherent waves results in interference phenomena which, however, can be observed directly only within the coherence volume. The dimensions of this coherence volume depend on the size of the radiation source, on the spectral width of the radiation and on the distance between source and observation point P.

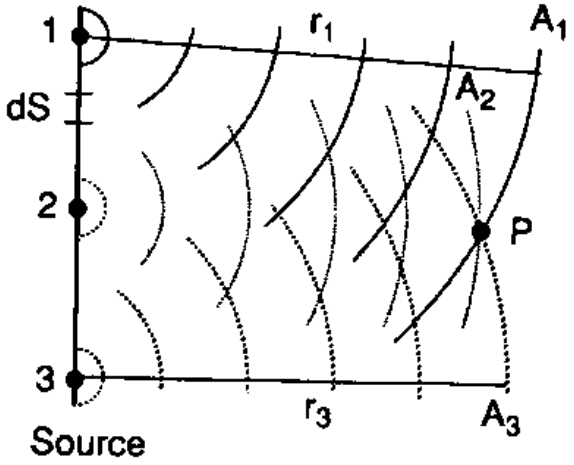

Fig.2.21. The field amplitudes A_n at a point P in a radiation field as superposition of an infinite number of waves from different surface elements dS_i of an extended source

Luce coerente può dare luogo a fenomeni di interferenza

COERENZA II

2.7.1 Temporal Coherence

Consider a point source PS in the focal plane of a lens forming a parallel light beam which is divided by a beam splitter S into two partial beams (Fig. 2.22). They are superimposed in the plane of observation B after reflection from the mirrors M_1, M_2. This arrangement is called a *Michelson interferometer* (Sect.4.2). The two beams with wavelength λ travel different optical path lengths SM_1SB and SM_2SB, and their path difference in the plane B is

$$\Delta s = 2(SM_1 - SM_2) .$$

The mirror M_2 is mounted on a carriage and can be moved, resulting in a continuous change of Δs. In the plane B, one obtaines maximum intensity when both amplitudes have the same phase, which means $\Delta s = m\lambda$, and minimum intensity if $\Delta s = (2m+1)\lambda/2$. With increasing Δs, the contrast $(I_{max}-I_{min})/(I_{max}+I_{min})$ decreases and vanishes if Δs becomes larger than the coherence length Δs_c (Sect.2.7.4). Experiments show that Δs_c is related to the spectral width $\Delta\omega$ of the incident wave by

$$\Delta s_c \simeq c/\Delta\omega = c/(2\pi\Delta\nu) . \quad (2.90)$$

Lunghezza di coerenza

This observation may be explained as follows. A wave emitted from a point source with the spectral width $\Delta\omega$ can be regarded as a superposition of many quasi-monochromatic components with frequencies ω_n within the interval $\Delta\omega$. The superposition results in wave trains of finite length $\Delta s_c = c\Delta t = c/\Delta\omega$ because the different components with slightly different frequencies ω_n come out of phase during the time interval Δt and interfere destructively causing the total amplitude to decrease (Sect.3.1). If the path difference Δs in the Michelson interferometer becomes larger than Δs_c, the split wave trains no longer overlap in the plane B. The coherence lengths Δs_c of a light source therefore becomes larger with decreasing spectral width $\Delta\omega$.

Example 2.8

a) A low-pressure mercury spectral lamp with a spectral filter which only transmits the green line $\lambda = 546$ nm has, because of the Doppler width $\Delta\omega_D = 4\cdot10^9$ Hz, a coherence length of $\Delta s_c \simeq 8$ cm.

b) A single-mode HeNe laser with a bandwidth of $\Delta\nu = 1$ MHz has a coherence length of about 50 m.

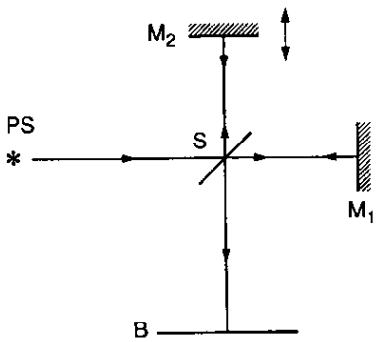

Fig.2.22. Michelson interferometer for measurements of the temporal coherence of radiation from the source S

Coerenza temporale del fascio essenziale per misure di interferometria Ad esempio: misure dimensionali (non invasive) di componenti meccanici con precisione nanometrica

Coerenza spaziale richiede monocromaticità!

PROFILOMETRIA OTTICA

Estensione tecniche interferometriche al caso 2D: profilometria ottica (senza contatto)

Non-contact profilometers [edit]

An optical profilometer is a non-contact method for providing much of the same information as a stylus based profilometer. There are many different techniques which are currently being employed, such as laser triangulation (triangulation sensor), confocal microscopy and digital holography.

Advantages of optical profilometers

- Speed: Because the non-contact profilometer does not touch the surface the scan speeds are dictated by the light reflected from the surface and the speed of the acquisition electronics.
- Reliability: optical profilometers do not touch the surface and therefore cannot be damaged by surface wear or careless operators. Many non-contact Profilometers are solid-state which tends to reduce the required maintenance significantly.
- Spot size: The spot size, or lateral resolution, of optical methods ranges from a few micrometres down to sub micrometre.

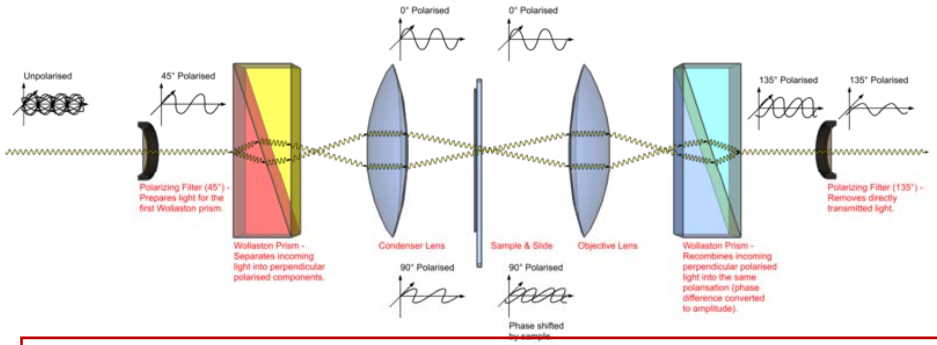

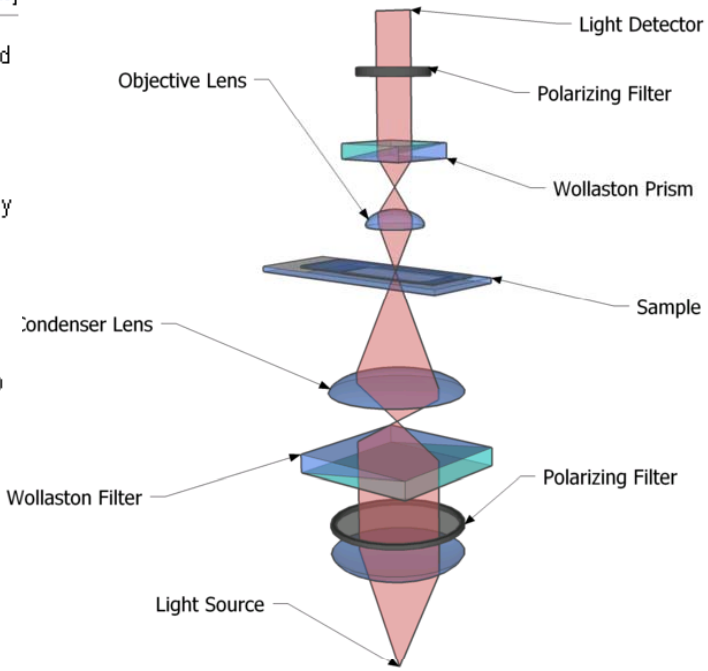

Microscopio Nomarski

Due fasci hanno diverso cammino ottico dipendente da posizione → sensibilità fase (essenziale usare fasci coerenti)

Altre tecniche possibili con fasci coerenti: microscopia confocale, ellissometria, etc.

COERENZA III

2.7.2 Spatial Coherence

The radiation from an *extended source* LS of size b illuminates two slits S_1 and S_2 in the plane A a distance d apart (Young's double-slit interference experiment, Fig.2.23a). The total amplitude and phase at each of the two slits are obtained by superposition of all partial waves emitted from the different surface elements df of the source, taking into account the different paths df-S_1 and df-S_2.

The intensity at the point of observation P in the plane B depends on the path difference S_1P-S_2P and on the phase difference $\Delta\phi = \phi(S_1)-\phi(S_2)$ of the total field amplitudes in S_1 and S_2. If the different surface elements df of the source emit independently with random phases (thermal radiation source) the phases of the total amplitudes in S_1 and S_2 will also fluctuate randomly. However, this would not influence the intensity in P as long as these fluctuations occur in S_1 and S_2 synchronously, because then the phase difference $\Delta\phi$ would remain constant. In this case, the two slits form two coherent sources which generate an interference pattern in the plane B.

For radiation emitted from the central part 0 of the light source this proves to be true since the paths $0S_1$ and $0S_2$ are equal and all phase fluctuations in 0 arrive simultaneously in S_1 and S_2. For all other points Q of the source, however, path differences $\Delta s_Q = QS_1 - QS_2$ exist, which are largest for the edges R of the source. From Fig.2.23b one can infer for b << r the relation

$$\Delta s_R = R_1S_2 - R_1S_1 = R_2S_1 - R_1S_1 \simeq b\sin(\theta/2) .$$

For $\Delta s_R > \lambda/2$ the phase difference $\Delta\phi$ of the partial amplitudes in S_1 and S_2 exceeds π. With random emission from the different surface elements df of the source, the time-averaged interference pattern in the plane B will be washed out. The condition for coherent illumination of S_1 and S_2 from a light source with the dimension b is therefore

$$\Delta s = b\sin(\theta/2) < \lambda/2 .$$

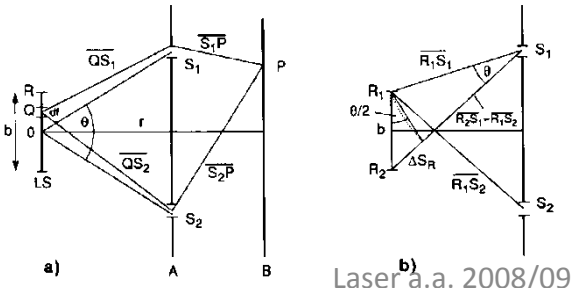

Fig.2.23a,b. Young's double-slit arrangement for measurements of spatial coherence

With $2\sin(\theta/2) = d/r$, this condition can be written as

$$bd/r < \lambda . \qquad (2.91a)$$

Extension of this coherence condition to two dimensions yields for a source area $A_s = b^2$ the following condition for the maximum surface $A_c = d^2$ which can be illuminated coherently:

$$b^2d^2/r^2 \leq \lambda^2 . \qquad (2.91b)$$

Since $d\Omega = d^2/r^2$ is the solid angle accepted by the illuminated surface $A_c = d^2$ this can be formulated as

$$A_s d\Omega \leq \lambda^2 . \qquad (2.91c)$$

The source surface $A_s = b^2$ determines the maximum solid angle $d\Omega \leq \lambda^2/A_s$ inside which the radiation field shows spatial coherence. Equation (2.91c) reveals that radiation from a point source (spherical waves) is spatially coherent within the whole solid angle $d\Omega = 4\pi$. The coherence surfaces are spheres with the source in the center. Likewise, a plane wave produced by a point source in the focus of a lens shows spatial coherence over the whole aperture confining the light beam. For given source dimensions, the coherence surface $A_c = d^2$ increases with the square of the distance from the source. Because of the vast distances to stars, the starlight received by telescopes is spatially coherent across the telescope aperture in spite of the large diameter of the radiation source.

The arguments above may be summarized as follows: The coherence surface S_c, i.e., that maximum area A_c which can be coherently illuminated at a distance r from an extended quasi-monochromatic light source with the area A_s emitting at a wavelength λ is determined by

$$S_c = \lambda^2 r^2/A_s . \qquad (2.92)$$

Superficie di coerenza

Superficie di coerenza: area che può essere illuminata con luce coerente

COERENZA IV

2.7.3 Coherence Volume

With the coherence length $\Delta s_c = c/\Delta\omega$ in the propagation direction of the radiation with the spectral width $\Delta\omega$ and the coherence surface $S_c = \lambda^2 r^2/A_s$ the coherence volume $V_c = S_c \Delta s_c$ becomes

$$V_c = \frac{\lambda^2 r^2 c}{\Delta\omega A_s} . \qquad (2.93)$$

Volume di coerenza

A unit surface element of a source with the spectral radiance L_ω [W/m^2·sterad] emits within the frequency interval $d\omega = 1$ Hz $L_\omega/\hbar\omega$ photons per second into the unit solid angle 1 sterad.

The mean number $\bar{n}$ of photons in the spectral range $\Delta\omega$ within the coherence volume defined by the solid angle $\Delta\Omega = \lambda^2/A_s$ and the coherence length $\Delta s_c = c\Delta t_c$ generated by a source with area A_s is therefore

$$\bar{n} = (L_\omega/\hbar\omega) A_s \Delta\Omega \Delta\omega \Delta t_c .$$

With $\Delta\Omega = \lambda^2/A_s$ and $\Delta t_c \simeq 1/\Delta\omega$ this gives

$$\bar{n} = (L_\omega/\hbar\omega)\lambda^2 . \qquad (2.94)$$

Example 2.9

For a thermal radiation source, the spectral radiance for linearly polarized light [(2.25) divided by a factor 2] is for $\cos\phi = 1$ and $L_\nu d\nu = L_\omega d\omega$

$$L_\nu = \frac{h\nu^3/c^2}{e^{h\nu/kT} - 1} .$$

The mean number of photons within the coherence volume is then with $\lambda = c/\nu$

$$\bar{n} = \frac{1}{e^{h\nu/kT} - 1} .$$

Esempio: sorgente termica (corpo nero)

This is identical to the mean number of photons per mode of the thermal radiation, as derived in Sect.2.2. Figure 2.5 and Example 2.3 give values of $\bar{n}$ for different conditions.

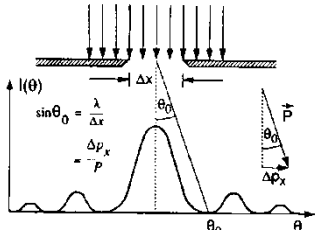

Fig.2.24. The uncertainty principle applied to the diffraction of light by a slit

The mean number $\bar{n}$ of photons per mode is often called the *degeneracy parameter* of the radiation field. This example shows that the coherence volume is related to the modes of the radiation field. This relation can be also illustrated in the following way:

If we allow the radiation from all modes with the same direction of $\mathbf{k}$ to escape through a hole in the cavity wall with the area $A_s = b^2$, the wave emitted from A_s will not be strictly parallel but will have a diffraction-limited divergence angle $\theta \simeq \lambda/b$ around the direction of $\mathbf{k}$. This means that the radiation is emitted into a solid angle $d\Omega = \lambda^2/b^2$. This is the same solid angle (2.91c) which limits the spatial coherence.

The modes with the same direction of $\mathbf{k}$ (which we assume to be the z direction) may still differ in $|\mathbf{k}|$, i.e., they may have different frequencies ω. The coherence length is determined by the spectral width $\Delta\omega$ of the radiation emitted from A_s. Since $|\mathbf{k}| = \omega/c$ the spectral width $\Delta\omega$ corresponds to an interval $\Delta k = \Delta\omega/c$ of the k values. This radiation illuminates a minimum "diffraction surface"

$$A_D = r^2 d\Omega = r^2\lambda^2/A_s .$$

Multiplication with the coherence length $\Delta s_c = c/\Delta\omega$ yields again the coherence volume $V_c = A_D c/\Delta\omega = r^2\lambda^2 c/(\Delta\omega A_s)$ of (2.93). We shall now demonstrate that the coherence volume is identical with the spatial part of the elementary cell in the general phase space.

As is well known from atomic physics, the diffraction of light can be explained by Heisenberg's uncertainty relation. Photons passing through a slit of width Δx have the uncertainty Δp_x of the x component p_x of their momentum $\mathbf{p}$, given by $\Delta p_x \Delta x \geq \hbar$ (Fig.2.24).

Generalized to three dimensions, the uncertainty principle postulates that the simultaneous measurements of momentum and location of a photon has the minimum uncertainty

$$\Delta p_x \Delta p_y \Delta p_z \Delta x \Delta y \Delta z \geq \hbar^3 = V_{ph} , \qquad (2.95)$$

where $V_{ph} = \hbar^3$ is the volume of one cell in phase space. *Photons within the same cell of the phase space are indistinguishable and can be therefore regarded as identical.*

Photons which are emitted from the hole $A_s = b^2$ within the diffraction angle $\theta = \lambda/b$ against the surface normal (Fig.2.25), which may point into the z direction, have the minimum uncertainty

$$\Delta p_x = \Delta p_y = |\mathbf{p}|\lambda/(2\pi b) = (\hbar\omega/c)\lambda/(2\pi b) = (\hbar\omega/c)d/(2\pi r) , \qquad (2.96)$$

of the momentum components p_x and p_y (the last equality follows from (2.91b).

COERENZA V

The uncertainty Δp_z is mainly caused by the spectral width $\Delta\omega$. Since $p = \hbar\omega/c$, we find

$$\Delta p_z = (\hbar/c)\Delta\omega \,. \qquad (2.97)$$

Substituting (2.96,97) into (2.95) we obtain for the spatial part of the phase-space cell

$$\Delta x \Delta y \Delta z = \frac{\lambda^2 r^2 c}{\Delta\omega A_s} = V_c \,,$$

which turns out to be identical with the coherence volume defined by (2.93).

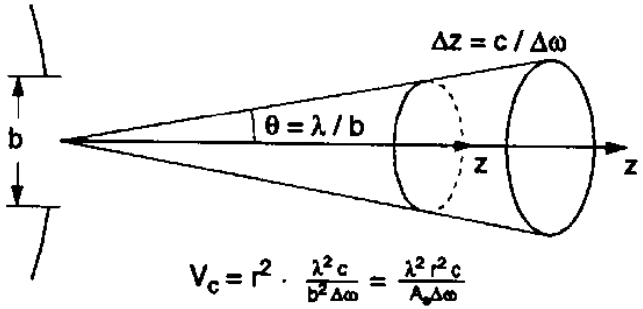

Fig.2.25. Coherence volume and phase space cell

44

Volume di coerenza rappresenta regione (spaziale) in cui i fotoni si comportano allo stesso modo

Rozzamente, volume di coerenza dipende da:
- Area di coerenza ← spazio delle fasi reale
- Lunghezza di coerenza ← tempo coerenza ← monocromaticità

Fotoni emessi da piccolo volume di mezzo attivo per emissione stimolata appartengono alle stesse celle dello spazio delle fasci, cioè sono indistinguibili (quantisticamente)

Nota: luce coerente può essere efficacemente focalizzata
(è un time reversal rispetto alla generazione), con il solo limite della diffrazione

BRILLANZA

1.4.4. Brightness

We define the brightness of a given source of em waves as the power emitted per unit surface area per unit solid angle. To be more precise let dS be the elemental surface area at point O of the source (Fig. 1.7a). The power dP emitted by dS into a solid angle $d\Omega$ around direction OO' can be written as:

$$dP = B \cos\theta \, dS \, d\Omega \tag{1.4.3}$$

where θ is the angle between OO' and the normal $\mathbf{n}$ to the surface. Note that the factor $\cos\theta$ occurs because the physically important quantity for emission along the OO' direction is the projection of dS on a plane orthogonal to the OO' direction, i.e., $\cos\theta \, dS$. The quantity B defined through Eq. (1.4.3) is called the *source brightness* at point O in the direction OO'. This quantity generally depends on polar coordinates θ and ϕ of the direction OO' and on point O. When B is a constant, the source is said to be isotropic (or a Lambertian source).

Let us now consider a laser beam of power P, with a circular cross section of diameter D and with a divergence θ (Fig. 1.7b). Since θ is usually very small, we have $\cos\theta \cong 1$. Since the area of the beam is equal to $\pi D^2/4$ and the emission solid angle is $\pi\theta^2$, then, according to Eq. (1.4.3), we obtain the beam brightness as:

$$B = \frac{4P}{(\pi D\theta)^2} \tag{1.4.4}$$

Note that, if the beam is diffraction limited, we have $\theta = \theta_d$, and, with the help of Eq. (1.4.1), we obtain from Eq. (1.4.4):

$$B = \left(\frac{2}{\beta\pi\lambda}\right)^2 P \tag{1.4.5}$$

β : fattore geometrico ~ 1

which is the maximum brightness for a beam of power P.

Brightness is the most important parameter of a laser beam and, in general, of any light source. To illustrate this point we first recall that, if we form an image of any light source through a given optical system and if we assume that the object and image are in the same medium (e.g., air), then the following property holds: The brightness of the image is always less than or equal to that of the source, the equality holding when the optical system provides lossless imaging of the light emitted by the source. To illustrate further the importance of

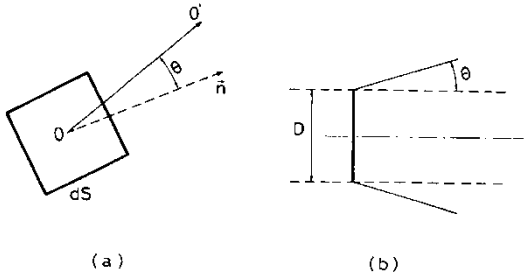

FIG. 1.7. (a) Surface brightness at the point O for a general source of em waves. (b) Brightness of a laser beam of diameter D and divergence θ.

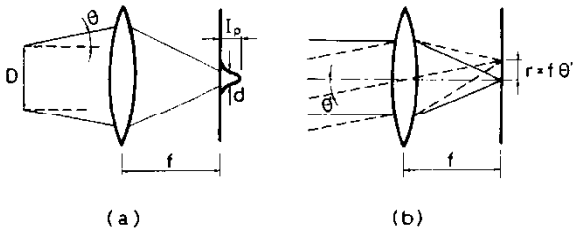

FIG. 1.8. (a) Intensity distribution in the focal plane of a lens for a beam of divergence θ. (b) Plane wave decomposition of the beam in (a).

brightness, let us consider the beam in Fig. 1.7b, with divergence equal to θ, to be focused by a lens of focal length f. We are interested in calculating the peak intensity of the beam in the focal plane of the lens (Fig. 1.8a). To make this calculation we recall that the beam can be decomposed into a continuous set of plane waves with an angular spread of approximately θ around the propagation direction. Two such waves, making an angle θ', are indicated by solid and dashed lines, respectively, in Fig. 1.8b. The two beams are each focused on a distinct spot in the focal plane, and, for a small angle θ', the two spots are transversly separated by a distance $r = f\theta'$. Since the angular spread of the plane waves that make up the beam in Fig. 1.8a equals the beam divergence θ, we conclude that the diameter d of the focal spot in Fig. 1.8a is approximately equal to $d = 2f\theta$. For an ideal lossless lens, the overall power in the focal plane equals the power P of the incoming wave. The peak intensity in the focal plane is thus $I_p = 4P/\pi d^2 = P/\pi(f\theta)^2$. In terms of beam brightness, according to Eq. (1.4.4), we then have $I_p = (\pi/4)B(D/f)^2$. Thus I_p increases with increasing beam diameter D. The maximum value of I_p is then attained when D is made equal to the lens diameter D_L. In this case we obtain

$$I_p = \left(\frac{\pi}{4}\right)(N.A.)^2 B \tag{1.4.6}$$

where $N.A. = \sin[\tan^{-1}(D_L/f)] \cong (D_L/f)$ is the lens numerical aperture. Equation (1.4.6) then shows that, for a given numerical aperture, the peak intensity in the focal plane of a lens depends only on beam brightness.

A laser beam of even moderate power (e.g., a few milliwatts) has a brightness several orders of magnitude greater than that of the brightest conventional sources (see, e.g., Problem 1.7). This is mainly due to the highly directional properties of the laser beam. According to Eq. (1.4.6) this means that the peak intensity produced in the focal plane of a lens can be several orders of magnitude greater for a laser beam compared to that of a conventional source. Thus the intensity of a focused laser beam can reach very large values, a feature exploited in many applications of lasers.

Es.: HeNe, 1mW, 633nm: B~10^9 W/m^2
I_P>10^4 W/cm^2~$3x10^{22}$ fotoni/(s cm^2)
[>> densità superficiale tipica materia]

POTENZA ED INTENSITÀ LASER

Molte applicazioni dei laser dipendono da elevate intensità
Oltre a coerenza (direzionalità e possibilità di focalizzare), intensità dipende da carattere amplificatore di mezzo attivo

Potenze *tipiche* di alcuni laser CW (in continua):
-HeNe: 1-50 mW
-Ar^+: 0.1-10 W
-CO_2: 10 W- kW
-Nd:YAG (e simili): 5-50 W
-Diodo: 10 mW – 10 W ("barrette")

Limitazioni tecnologiche per la potenza:
- Efficienza pompaggio (valori tipici 1-10%);
- Complicati sistemi accessori (raffreddamento, alimentazione, controllo, etc.);
- Densità del mezzo attivo (al massimo idealmente vengono emessi n/τ fotoni/(volume secondo)
- Volume del mezzo attivo (conviene sia piccolo per aumentare coerenza spaziale)
- Robustezza del mezzo attivo (il mezzo attivo è interessato da potenze paragonabili a quelle di emissione)

Limitazione fisica per la potenza:
$-\Delta N \rightarrow \Delta N_{thr}$ in condizioni stazionarie
→ guadagno tende a un limite

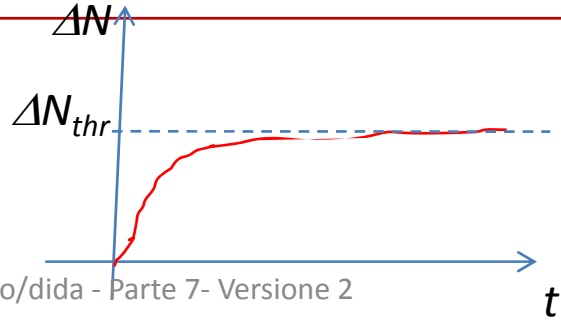

LASER DI INTENSITÀ STRAORDINARIA

Richiesta di sorgenti laser sempre più intense: applicazioni *ordinarie* (e.g., trattamento materiali) o straordinarie (esempio: fusione inerziale, plasmi densi, etc.)

Fusione Termonucleare controllata

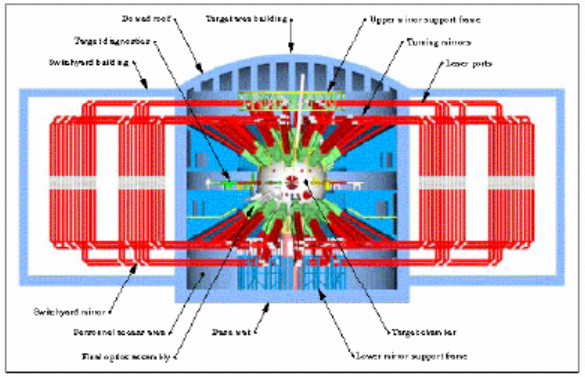

Nd:vetr
2 MJ
10 ns
200 fas

λ =1.3 μm τ = 450 psec E = 1500 J

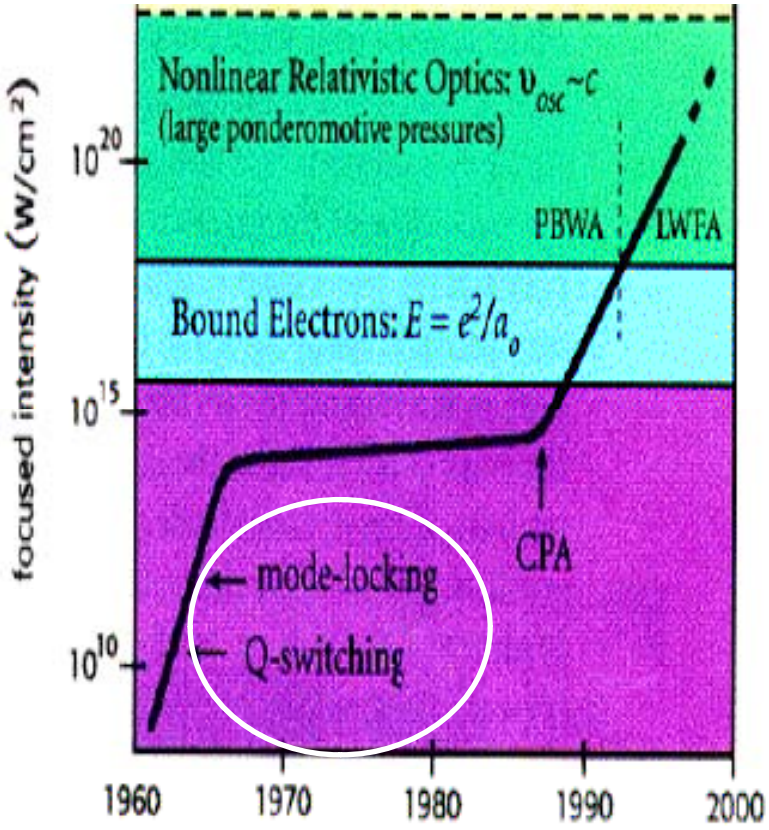

Figure 1. Laser intensity as a function of year, showing the impact of the CPA concept and the different thresholds of physical regimes. The sharp increase in intensity since the advent of CPA is comparable to the sharp increase after the invention of the laser in the 1960's.

Spesso necessarie sorgenti con funzionamento impulsato

LASER IMPULSATI

Funzionamento impulsato talvolta è inevitabile per:
-ragioni tecnologiche (e.g., facilità innesco scarica in miscele gassose, disponibilità lampade flash, etc.)
-Specifiche pompaggio (e.g., laser ad eccimeri)

Talvolta funzionamento impulsato studiato specificamente per aumentare intensità

Parametro importante per laser impulsati: energia per impulso ($E = N_{pulse} h\nu$)
La potenza di picco $P_{peak}=E/t$ può diventare gigante se t è molto piccolo!
La potenza media $P=E\,f$ può rimanere ragionevolmente piccola

Es.: laser eccimeri XeCl:, 308 nm, commerciale:
E= 0.5 J, t = 20 ns, f = 100 Hz → P_{peak}= $2.5x10^7$ W, P = 50 W (ed N_{pulse}~10^{18} fotoni)

Frequenza di ripetizione	f
CW, 100 MHz, kHz, Hz, single shot	
Potenza Media	P
mW → W → kW	
Energia per impulso	E = P/f
pJ → mJ → J → kJ	
Durata impulso	t
µs → ns → ps → fs	
Potenza di Picco	P_o = E / t
MW → GW → TW	
Intensità	I = P / S
$mW/cm^2 \rightarrow 10^{18}$ W/cm^2	

Q-SWITCHING I

8.4. Q-SWITCHING

In Chap. 7 we saw that, under cw operation, the population inversion is fixed at its threshold value when oscillation starts. Even under the pulsed operating conditions considered in Sect. 8.2, the population inversion is seen to exceed the threshold value by only a relatively small amount (see Fig. 8.1), due to the onset of stimulated emission. Suppose now that a shutter is introduced into the laser cavity. If the shutter is closed, laser action is prevented, so the value of the population inversion may far exceed the threshold population holding when the shutter is absent. If the shutter is now opened suddenly, the laser will exhibit a gain that greatly exceeds losses; stored energy may then be released in the form of a short and intense light pulse.[8] Since this operation involves switching the cavity Q-factor from a low to a high value, the technique is usually called *Q-switching*. This technique allows one to generate laser pulses with a duration comparable to the photon decay time (i.e., from a few nanoseconds to a few tens of nanoseconds) and high-peak power (in the megawatt range).

8.4.1. Dynamics of the Q-Switching Process

To describe the Q-switching dynamic behavior, we assume that a step pump pulse is applied to the laser starting at time $t = 0$, i.e., $R_p(t) = 0$ for $t < 0$ and $R_p(t) = R_p$ = constant for $0 < t < t_p$; meanwhile the shutter is closed (Fig. 8.3a). For $0 < t < t_p$, the time behavior of the population inversion can be calculated from Eq. (7.2.16a), for a four-level laser, or

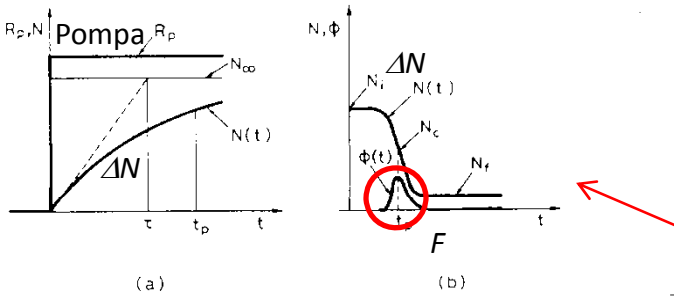

FIG. 8.3. Sequence of events in a Q-switched laser: (a) Idealized time behavior of the pump rate, R_p, and of the population inversion, N, before Q-switching. (b) Time behavior of population inversion, N, and photon number, ϕ, after Q-switching (fast switching case.)

from Eq. (7.2.24a), for a quasi-three-level laser, with ϕ set to zero. For instance, for a four-level laser, we obtain

$$N(t) = N_\infty[1 - \exp(-t/\tau)] \tag{8.4.1}$$

where the asymptotic value N_∞ is given by:

$$N_\infty = R_p\tau \tag{8.4.2}$$

as we readily obtain from Eq. (7.2.16a) by setting $dN/dt = 0$. The time behavior of $N(t)$ is also shown in Fig. 8.3a. From Eq. (8.4.1) and Fig. 8.3a we see that the duration t_p of the pump pulse ideally should be comparable to, or shorter than, the upper state lifetime τ. In fact, for $t_p \gg \tau$, $N(t)$ does not undergo any further appreciable increase and the pump power, rather than being accumulated as inversion energy, would be wasted through spontaneous decay. From Eq. (8.4.2) we also see that, to achieve a sufficiently large inversion, a long lifetime τ is required. Thus Q-switching can be used, effectively, with electric-dipole-forbidden laser transitions, where τ generally falls in the millisecond range. This is the case of most solid-state lasers (e.g., Nd, Yb, Er, Ho in different host materials; Cr-doped materials, such as alexandrite, Cr:LiSAF, and ruby) and some gas lasers (e.g., CO_2 or iodine). On the other hand, for semiconductor lasers, dye lasers, and a number of important gas lasers (e.g., He-Ne, Ar, Excimers), the laser transition is electric-dipole allowed and the lifetime is on the order of a few to a few tens of nanoseconds. In this case, with the usual values for pump rates R_p available, the achievable inversion N_∞ is too low to be of interest for Q-switching.

We now assume that the shutter is suddenly opened at time $t = t_p$, so that cavity loss $\gamma(t)$ is switched from a very high value, corresponding to a closed shutter, to the value γ for the same cavity with the shutter open (*fast switching*). We now take the time origin at the instant when switching occurs (Fig. 8.3b). The time behavior of the population inversion $N(t)$ and the number of photons $\phi(t)$ can then be obtained from the rate equations with the simplifying assumption that, during the short time of the Q-switching process, the effect of the decay term N/τ can be neglected. The qualitative behavior of $N(t)$ and $\phi(t)$ can then be depicted as in Fig. 8.3b. The population inversion starts from the initial value N_i, which can be obtained from Eq. (8.4.1) for $t = t_p$, then remains constant for some time, and finally begins to be depleted when the cavity photon number reaches a sufficiently high value. When $N(t)$ eventually falls to the threshold inversion N_c, the photon number reaches its peak value, as discussed earlier for the case of relaxation oscillations in Sect. 8.2. From this time on, the laser exhibits net loss rather than net gain; as a consequence, the photon number decreases to zero. During the same time the population inversion decreases to a final value N_f, which is left in the active medium; its value is established by the dynamics of the Q-switching process (see Sect. 8.4.4). Note that the time scales in Figs. 8.3a–b are very different; in fact, the time scale in Fig. 8.3a is established by the value of the upper state lifetime and thus corresponds to the microsecond range (usually, 100 μs–1 ms). The time scale in Fig. 8.3b, on the other hand, turns out to be of the order of the cavity photon decay time (see Sect. 8.4.4) and hence falls in the nanosecond range (usually, 5–50 ns).

So far we have considered the dynamic behavior corresponding to fast switching, where the switching of cavity loss is treated as instantaneous. In practice, fast switching requires

Q-switching: la cavità è “temporizzata”
Maggiore energia incameratain mezzo attivo

Q-SWITCHING II

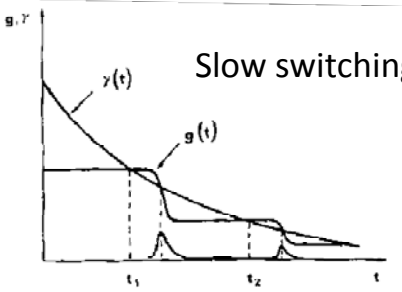

FIG. 8.4. Sequence of events in the slow switching case demonstrating the occurrence of multiple pulses. In the figure, $g(t) = \sigma N(t)l$, where l is the length of the active medium, represents the laser gain.

their peak value (several photon decay times, i.e., typically from a few tens to a few hundreds of a nanosecond). In the case of *slow switching*, the dynamic behavior is somewhat more complicated and multiple pulses may result. Figure 8.4 depicts this behavior, where cavity loss $\gamma(t)$ is assumed to decay from its initially high value to a final value in a relatively long time. The same figure also shows the corresponding time behavior of the single-pass gain $g(t) = \sigma N l$ and the cavity photon number $\phi(t)$. The first pulse starts at time t_1 when the decreasing loss $\gamma(t)$ equals the instantaneous gain $g(t)$. The pulse then reaches its peak value when the gain, owing to its decrease due to saturation, equals the loss. After this first pulse, the gain is driven below the loss, so further oscillation cannot occur until the switch opens further, thus decreasing the loss below the gain. A second pulse can then be produced (occurring at time t_2 in the figure) whose peak again occurs when gain saturation makes the gain equal to loss.

8.4.2. Q-Switching Methods

Several methods have been developed to achieve switching of the cavity Q; in this section we limit ourselves to discussing the most commonly used, namely:[9] (1) Electro-optical shutters. (2) Rotating prisms. (3) Acoustooptical switches. (4) Saturable absorbers. These devices are generally grouped into two categories, *active* and *passive Q-switches*. In an active Q-switching device, some external active operation must be applied to this device (e.g., a change of the voltage applied to the electrooptical shutter) to produce Q-switching. In a passive Q-switch, the switching operation is automatically produced by the optical nonlinearity of the element used (e.g., a saturable absorber).

8.4.2.1. Electrooptical Q-Switching

These devices use a cell exploiting an electrooptical effect, usually the Pockels effect, to induce Q-switching. A cell based on the Pockels effect (*Pockels cell*) consists of a suitable nonlinear crystal, such as KD*P or lithium niobate for the visible-to-near-infrared region or cadmium telluride for the middle-infrared, in which an applied dc voltage induces a change in the crystal's refractive indices. This induced birefringence turns out to be proportional to the applied voltage. Figure 8.5a shows a Q-switched laser using a suitable combination of a polarizer and a Pockels cell. The Pockels cell is oriented and biased so that the x- and y-axes of the induced birefringence lie in the plane orthogonal to the resonator axis. The polarizer axis then makes a 45° angle to the birefringence axes.

Consider now a laser beam propagating from the active medium toward the polarizer–Pockels cell combination with polarization parallel to the polarizer axis. Ideally this beam is totally transmitted by the polarizer and then incident on the Pockels cell. The E-field of the incoming wave is at 45° to the birefringence x- and y-axes of the Pockels cell and it can be resolved into components E_x and E_y (Fig. 8.5b) with their oscillations in phase. After passing through the Pockels cell, these two components have experienced different phase shifts, giving rise to the phase difference:

$$\Delta\varphi = k\Delta n L' \tag{8.4.3}$$

Sfasamento (ritardo) tra componenti *E*

where $k = 2\pi/\lambda$, $\Delta n = n_x - n_y$ is the value of the induced birefringence, and L' is the crystal length. If the voltage applied to the Pockels cell is such that $\Delta\varphi = \pi/2$, then the two field components leaving the Pockels cell differ in phase by $\pi/2$. This means that when E_x is maximum, E_y is zero and vice versa; i.e., the wave is circularly polarized (Fig. 8.5c). After reflection at the mirror, the wave passes once more through the Pockels cell, so its x- and y-components acquire an additional $\Delta\varphi = \pi/2$ phase difference. The total phase difference then becomes π, so that, when, e.g., E_x is at its maximum (positive) value, E_y is at its maximum (negative) value, as shown in Fig. 8.5d. As a result, the overall field E is again linearly polarized but with a polarization axis at 90° to that of the original wave in Fig. 8.5b. This beam is therefore not transmitted by the polarizer, but instead it is reflected out of the cavity (see Fig. 8.5a). This condition corresponds to the Q-switch being closed. The switch is then opened by removing the bias voltage to the Pockels cell. In this case the induced

Tempi di risposta tipici ~ ns

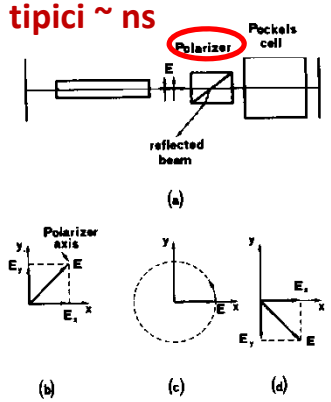

FIG. 8.5. (a) Possible polarizer-Pockels-cell combination for Q-switching. Figures (b), (c), and (d) show the E-field components along the birefringence axes of the Pockels cell in a plane orthogonal to the resonator axis.

Pockel effect: switch rapido della polarizzazione attraverso birifrangenza (sfasamento tra componenti del campo)

Q-SWITCHING III

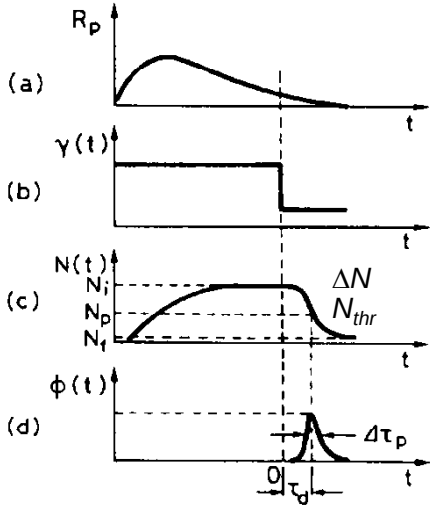

falls in the millisecond range, while the time scale for events when $t > 0$ falls in the nanosecond range. Q-switched lasers with a pulsed pump can obviously be operated repetitively; the typical repetition rates range from a few to a few tens of Hz. (2) *Continuously pumped, repetitively Q-switched operation* (Fig. 8.10), where a cw pump R_p is applied to the laser (Fig. 8.10a) and cavity losses are periodically switched from a high to a low value (Fig. 8.10b). Laser output then consists of a continuous train of Q-switched pulses (Fig. 8.10c). During each pulse, inversion falls from its initial value N_i (before Q-switching) to a final value N_f (after the Q-switched pulse; see Fig. 8.10d). The population inversion is then restored to its initial value N_i by the pumping process before the next Q-switching event. Since the time taken to restore the inversion is roughly equal to the upper-state

FIG. 8.9. Development of a Q-switched laser pulse in pulsed operation. The figure shows the time behavior of: (a) the pump rate R_p; (b) the resonator loss γ; (c) the population inversion N; (d) the number of photons ϕ.

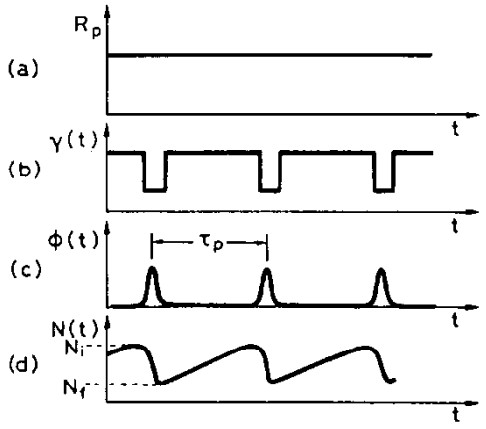

FIG. 8.10. Development of Q-switched laser pulses in a repetitively Q-switched, cw pumped laser. The figure shows the time behavior of: (a) the pump rate R_p; (b) the resonator losses γ; (c) the number of photons ϕ; (d) the population inversion N.

Q-switching applicabile in condizioni di pompa impulsata (più frequente) o pompa CW

Esempi tipici:
-pompa impulsata Nd:YAG, E~ 0.1 – 1 J, t~10ps –10ns
-pompa CW: Ar^+, E ~ 10 – 100 mJ, t~1–100ns

MODE-LOCKING I

8.6. MODE LOCKING

Let us now consider a laser oscillating in a large number of longitudinal modes. Under ordinary circumstances, phases of these modes have random values, and, for cw oscillation beam, intensity shows random time behavior. Figure 8.15 shows the time behavior of the square of the electric field amplitude $|A(t)|^2$ of the output beam for $N = 51$ oscillating modes, each with the same amplitude E_0, and evenly separated in frequency by the frequency difference $\Delta\nu$ between consecutive longitudinal modes. The output beam is seen to consist of a random sequence of light pulses. Despite this randomness, since these pulses arise from the sum of N frequency components evenly spaced in frequency, the pulse waveform in Fig. 8.15 has the following features which are characteristics of a Fourier series: (1) The waveform is periodic with a period $\tau_p = 1/\Delta\nu$. (2) Each light pulse of the random waveform has a duration $\Delta\tau_p$ roughly equal to $1/\Delta\nu_L$, where $\Delta\nu_L = N\Delta\nu$ is the total oscillating bandwidth. Thus, for lasers with relatively large gain bandwidths, such as solid-state, dye, or semiconductor lasers, $\Delta\nu_L$ may be comparable to this bandwidth; hence short noise pulses with durations of picoseconds or less can be produced. Note that, since the response time of a conventional photodetector is usually much longer than a few picoseconds, we do not resolve this complex time behavior in the detected output of a random-phase, multimode laser; instead its average value is monitored. This value is the sum of powers in the modes; hence is proportional to NE_0^2.

Suppose now that the oscillating modes, while still having equal or comparable amplitudes, are somehow made to oscillate with some definite relation between their phases. Such a laser is referred to as mode locked, and the process by which modes are made to adopt a definite phase relation is referred to as *mode locking*.[15] Mode-locked lasers are considered at some length in the following sections.

Fluttuazioni in ampiezza tipiche di laser multimodo CW

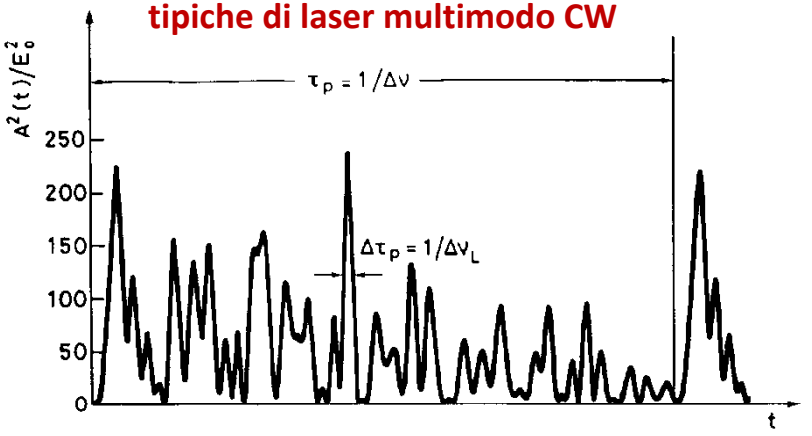

FIG. 8.15. Example of time behavior of the squared amplitude of the total electric field, $|A(t)|^2$, for the case of 51 oscillating modes, all with the same amplitude E_0 and with random phases.

Laser multimodo ordinario (CW) con larga forma di riga di guadagno: fotoni nei vari modi
La fase dei vari modi è random → fluttuazioni in ampiezza
Durata di ogni impulso di fluttuazione ~ $1/\Delta\nu_{laser}$ (cioè inverso di larghezza di guadagno)

MODE-LOCKING II

8.6.1. Frequency-Domain Description

We first describe mode-locking in the frequency domain and consider, as a first example, the case of $2n + 1$ longitudinal modes oscillating with the same amplitude E_0 (Fig. 8.16a). We assume that phases φ_l of the modes in the output beam to be locked according to the relation

$$\varphi_l - \varphi_{l-1} = \varphi \tag{8.6.1}$$

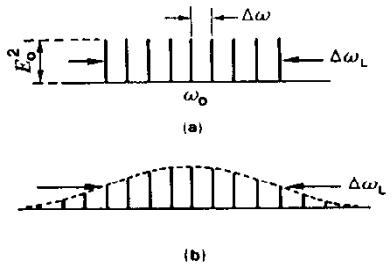

FIG. 8.16. Mode amplitudes (represented by vertical lines) versus frequency for a mode-locked laser. (a) Uniform amplitude distribution, and (b) Gaussian amplitude distribution, over a bandwidth (FWHM) $\Delta\omega_L$.

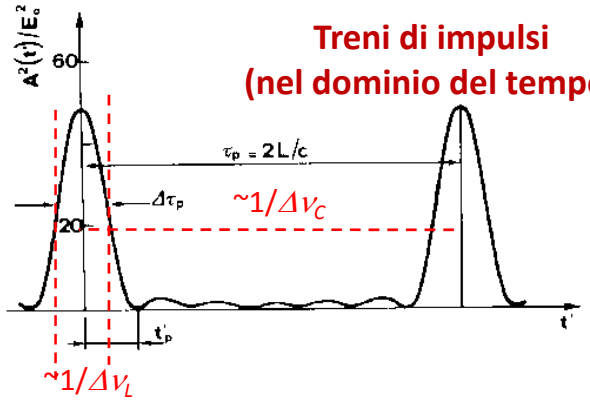

Treni di impulsi (nel dominio del tempo)

FIG. 8.17. Time behavior of the squared amplitude of the electric field for the case of seven oscillating modes with locked phases and equal amplitudes, E_0.

La presenza di molti modi di cavità (ognuno a frequenze diverse) produce impulsi nel dominio temporale

where φ is a constant. The total electric field $E(t)$ of the em wave at any given point in the output beam can be written as:

$$E(t) = \sum_{-n}^{+n} {}_l E_0 \exp\{ j[(\omega_0 + l\Delta\omega)t + l\varphi]\} \tag{8.6.2}$$

where ω_0 is the frequency of the central mode, $\Delta\omega$ is the frequency difference between two consecutive modes, and the value of the phase for the central mode has, for simplicity, been taken as zero. According to Eq. (8.6.2), the total electric field of the wave can be written as

$$E(t) = A(t) \exp(j\omega_0 t) \tag{8.6.3}$$

where

Analisi di Fourier

$$A(t) = \sum_{-n}^{+n} {}_l E_0 \exp[jl(\Delta\omega t + \varphi)] \tag{8.6.4}$$

Equation (8.6.3) shows that $E(t)$ can be represented in terms of a sinusoidal carrier wave, at the center mode frequency ω_0, whose amplitude $A(t)$ is time-dependent.

To calculate the time behavior of $A(t)$, we now change to a new time reference t' such that $\Delta\omega t' = \Delta\omega t + \varphi$. In terms of the new variable t', Eq. (8.6.4) can be transformed into:

$$A(t') = \sum_{-n}^{+n} {}_l E_0 \exp jl(\Delta\omega t') \tag{8.6.5}$$

The sum on the right-hand side is easily recognized as a geometric progression with a ratio $\exp j(\Delta\omega t')$ between consecutive terms. This progression is then easily summed to obtain

$$A(t') = E_0 \frac{\sin[(2n+1)\Delta\omega t'/2]}{\sin(\Delta\omega t'/2)} \tag{8.6.6}$$

Funzione di "diffrazione"

To understand the physical significance of Eq. (8.6.6), Fig. 8.17 shows the quantity $A^2(t')/E_0^2$, $A^2(t')$ being proportional to beam intensity, versus time t', for $2n + 1 = 7$ oscillating modes. As a result of the phase-locking condition (8.6.1), oscillating modes are seen to interfere so as to produce a train of evenly spaced light pulses. Pulse maxima occur when the denominator in Eq. (8.6.6) vanishes. In the new time reference t', the first maximum occurs for $t' = 0$. Note that, at this time, the numerator in Eq. (8.6.6) also vanishes. Making the approximation $\sin\alpha \cong \alpha$, which holds for small values of α, we readily see from Eq. (8.6.6) that $A^2(0) = (2n + 1)^2 E_0^2$. The next pulse occurs when the denominator in Eq. (8.6.6) again vanishes; this happens at time t' such that $(\Delta\omega t'/2) = \pi$. Two successive pulses are therefore separated by a time:

$$\tau_p = \frac{2\pi}{\Delta\omega} = \frac{1}{\Delta\nu} \tag{8.6.7}$$

Separazione temporale tra impulsi

where $\Delta\nu$ is the frequency separation between two consecutive modes. For $t' > 0$, the first zero for $A^2(t')$ in Fig. 8.17 occurs when the numerator in Eq. (8.6.6) again vanishes. This

MODE-LOCKING III

occurs at time t'_p such that $[(2n+1)\Delta\omega t'_p/2] = \pi$. Since the width $\Delta\tau_p$ (FWHM) of $A^2(t')$, i.e., of each laser pulse, is approximately equal to t'_p, we have

$$\Delta\tau_p \cong \frac{2\pi}{(2n+1)\Delta\omega} = \frac{1}{\Delta\nu_L} \tag{8.6.8}$$

Durata dell'impulso

where $\Delta\nu_L = (2n+1)\Delta\omega/2\pi$ is the total laser bandwidth (see Fig. 8.16a).

The mode-locking behavior in Fig. 8.17 can be readily understood if we represent field components in Eq. (8.6.5) by vectors in the complex plane. The *l*th amplitude component thus corresponds to a complex vector of amplitude E_0 rotating at the angular velocity $l\Delta\omega$. At time $t' = 0$ these vectors have zero phase [see Eq. (8.6.5)] and, accordingly, they lie in the same direction, which we assume to be the horizontal direction in Fig. 8.18. The total field in this case is $(2n+1)E_0$. For $t' > 0$, the vector corresponding to the central mode remains fixed; vectors for modes where $l > 0$, i.e., with $\omega > \omega_0$, rotate in one direction (e.g., counterclockwise), while vectors for modes where $\omega < \omega_0$ rotate in the opposite (clockwise) sense. Thus, in the case of, e.g., five modes, the situation at some later time t' will be as indicated in Fig. 8.18a. If now time t' is such that mode 1 has made a counterclockwise

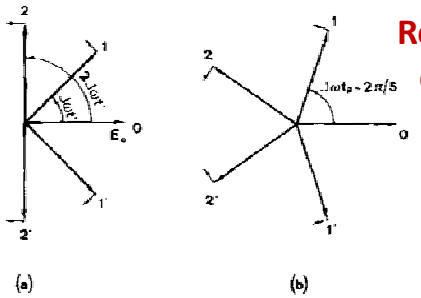

Relazione di fase e interferenza costruttiva

FIG. 8.18. Representation of the cavity mode amplitudes in the complex plane for the case of five modes. (a) shows the situation at a general time $t' > 0$, while (b) depicts the time instant at which the sum of the five mode amplitudes

rotation of 2π (which occurs when $\Delta\omega t' = 2\pi$), mode -1 will also have rotated (clockwise) by 2π, while modes 2 and -2 will have rotated by 4π. Therefore all these vectors are again aligned with the vector at frequency ω_0 and total field amplitude is again $(2n+1)E_0$. Thus the time interval τ_p between two consecutive pulses must be such that $\Delta\omega\tau_p = 2\pi$, as shown by Eq. (8.6.7). In this picture, the time t'_p at which $A(t')$ vanishes (see Fig. 8.17) corresponds to the situation where all vectors are evenly spaced around the 2π angle (Fig. 8.18b). To achieve this condition, mode 1 must have rotated only by $2\pi/5$ or, more generally for $(2n+1)$ modes, by $2\pi/(2n+1)$. The time duration t'_p and hence the pulse duration $\Delta\tau_p$ are thus given by Eq. (8.6.8).

Before proceeding we point out here some peculiar properties of mode-locked lasers. We first recall that, under the mode-locking condition given by Eq. (8.6.1), the output beam consists of a train of mode-locked pulses; the duration of each pulse $\Delta\tau_p$ is about equal to the inverse of the oscillating bandwidth $\Delta\nu_L$. This result is due to a general property of a Fourier series. Since $\Delta\nu_L$ can be of the order of the width of the gain line $\Delta\nu_0$, very short pulses (down to a few picoseconds) can be expected to result from mode-locking in solid-state or semiconductor lasers. For dye or tunable solid-state lasers, the gain linewidth can be at least a factor 100 times larger, so that much shorter pulse widths are possible and indeed have been obtained (e.g., ~ 25 fs for rhodamine 6G dye laser and ~ 7 fs for Ti:sapphire laser). In the case of gas lasers the gain linewidth is much narrower (up to a few GHz) so relatively long pulses are generated (to ~ 100 ps). Note also that the peak power of the pulse is proportional to $(2n+1)^2E_0^2$, whereas, for modes with random phases, average power is simply the sum of powers in the modes and hence proportional to $(2n+1)E_0^2$. Therefore, for the same number of oscillating modes and for the same field amplitudes E_0, the ratio between the peak-pulse power in the mode-locked case and the average power in the non-mode-locked case is equal to the number, $(2n+1)$, of oscillating modes, which for solid-state or liquid lasers, can be very high (10^3–10^4). Mode-locking is thus useful not only for producing pulses of very short duration but also for producing high peak powers.

So far we have restricted our considerations to the unrealistic case of an equal-amplitude mode spectrum (Fig. 8.16a). The spectral envelope is generally expected to have a bell shape, however, and, as a simple example, we consider a Gaussian shape (Fig. 8.16b). We can therefore write the amplitude E_l of the *l*th mode as:

$$E_l^2 = E_0^2 \exp[-(2l\Delta\omega/\Delta\omega_L)^2 \ln 2] \tag{8.6.9}$$

where $\Delta\omega_L$ represents the bandwidth (FWHM) of the spectral intensity. If we assume that phases are locked according to Eq. (8.6.1) and the phase of the central mode is zero, we find that $E(t)$ can be expressed as in Eq. (8.6.3), where the amplitude $A(t')$, in the time reference t', is given by:

$$A(t') = \sum_{-\infty}^{\infty} {}_lE_l \exp j(l\Delta\omega t') \tag{8.6.10}$$

If the sum is approximated by an integral [i.e., $A(t) \cong \int E_l \exp j(l\Delta\omega t)dl$], the field amplitude $A(t)$ is seen to be proportional to the Fourier transform of the spectral amplitude E_l. We then find that $A^2(t)$, i.e., the pulse intensity, is a Gaussian function of time, which can be written as

$$A^2(t) \propto \exp[-(2t/\Delta\tau_p)^2 \ln 2] \tag{8.6.11}$$

Durata degli impulsi può arrivare al fs (laser Ti:Sa)

Ti:Sa LASER

Laser con metalli di transizione (in cristalli)

La debole schermatura degli elettroni 3d negli ioni dei metalli di transizione porta a forti interazioni con i ligandi e può, quindi, dar luogo a bande molto larghe, con conseguente possibilità di accordabilità in frequenza molto ampia e generazione di impulsi ultra brevi. Esempi sono elencati in Tabella 3.3.

Laser	Crystal	Wavelength [nm]
Ruby	$Cr^{3+}:Al_2O_3$	694.4 692.9
Alexandrite	$Cr^{3+}:BeAl_2O_4$	700 - 800
Titanium-sapphire	$Ti^{3+}:Al_2O_3$	660-1180
Forsterite	$Cr^{3+}:Mg_2SiO_4$	1167-1345
Nickel-Magnesium	$Ni:MgF_2$	1610-1730
Cobalt-Magnesium	$Co:MgF_2$	1650-2010

Tabella 3.3. Alcuni laser con metalli di transizione e loro lunghezze d'onda di emissione

Ti: Zaffiro (Ti: Al_2O_3)

Il cristallo è drogato allo 0.1% con Titanio, il cui ione trivalente sostituisce quello dello Alluminio. L'effetto laser è stato scoperto nel 1982, ma i primi dispositivi sono stati resi commerciali solo nel 1988. Lavorano nel vicino infrarosso e tendono a sostituire i laser a coloranti rispetto ai quali mostrano maggiore stabilità, inferiore rumore e ampiezza di riga di circa 1kHz.

Laser a Ti:Sa (pompaggio simile a Nd:YAG et al.) ha enorme intervallo di guadagno
→Impulsi ultracorti facilmente ottenibili!

Pompaggio ottico, spesso con laser Ar^+ o diodo duplicato

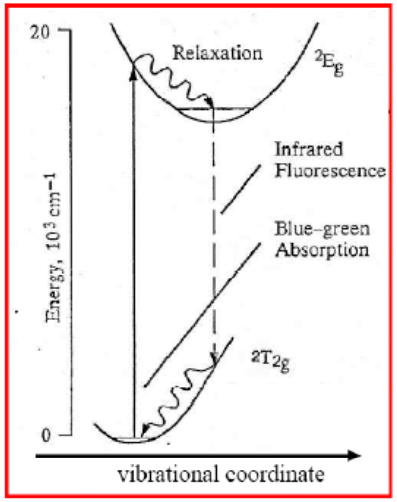

Ti:sapphire laser I

- 4-level laser
- Rapid vibronic relaxation in both upper & lower bands
- Stokes shift between emission & absorption profiles
- Upper laser level lifetime, 3μs.
- Stimulated emission cross-section $3x10^{-23}$ m^2

Ti:sapphire laser II

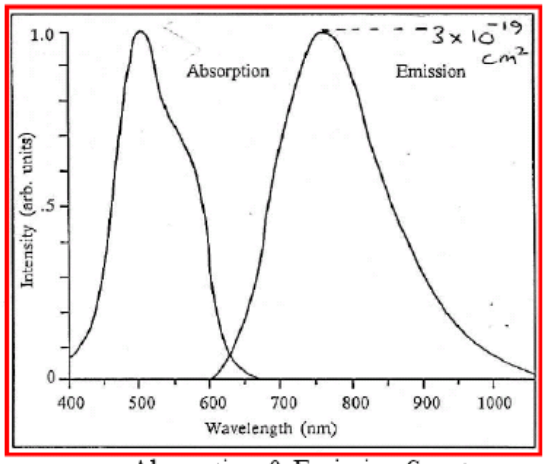

Absorption & Emission Spectra

METODI DI MODE-LOCKING

Active mode-locking

The most common active mode-locking technique places a standing wave acousto-optic modulator into the laser cavity. When driven with an electrical signal, this produces a sinusoidal amplitude modulation of the light in the cavity. Considering this in the frequency domain, if a mode has optical frequency ν, and is amplitude-modulated at a frequency f, the resulting signal has sidebands at optical frequencies $\nu-f$ and $\nu+f$. If the modulator is driven at the same frequency as the cavity-mode spacing $\Delta\nu$, then these sidebands correspond to the two cavity modes adjacent to the original mode. Since the sidebands are driven in-phase, the central mode and the adjacent modes will be phase-locked together. Further operation of the modulator on the sidebands produces phase-locking of the $\nu-2f$ and $\nu+2f$ modes, and so on until all modes in the gain bandwidth are locked. As said above, typical lasers are multi-mode and not seeded by a root mode. So multiple modes need to work out which phase to use. In a passive cavity with this locking applied there is no way to dump the entropy given by the original independent phases. This locking is better described as a coupling, leading to a complicated behavior and not clean pulses. Only because of the dissipative nature of the amplitude modulation the coupling is also dissipative, phase modulation would not work.

This process can also be considered in the time domain. The amplitude modulator acts as a weak *shutter* to the light bouncing between the mirrors of the cavity, attenuating the light when it is "closed", and letting it through when it is "open". If the modulation rate f is synchronised to the cavity round-trip time τ, then a single pulse of light will bounce back and forth in the cavity. The actual strength of the modulation does not have to be large; a modulator that attenuates 1 % of the light when "closed" will mode-lock a laser, since the same part of the light is repeatedly attenuated as it traverses the cavity.

Related to this amplitude modulation (AM) active mode-locking is frequency modulation (FM) mode-locking, which uses a modulator device based on the electro-optic effect. This device, when placed in a laser cavity and driven with an electrical signal, induces a small, sinusoidally varying frequency shift in the light passing through it. If the frequency of modulation is matched to the round-trip time of the cavity, then some light in the cavity sees repeated up-shifts in frequency, and some repeated down-shifts. After many repetitions, the up-shifted and down-shifted light is swept out of the gain bandwidth of the laser. The only light which is unaffected is that which passes through the modulator when the induced frequency shift is zero, which forms a narrow pulse of light.

The third method of active mode-locking is synchronous mode-locking, or synchronous pumping. In this, the pump source (energy source) for the laser is itself modulated, effectively turning the laser on and off to produce pulses. Typically, the pump source is itself another mode-locked laser. This technique requires accurately matching the cavity lengths of the pump laser and the driven laser.

Modulatore acusto-ottico (AOM):
Cristallo che supporta un'onda acustica (tipicamente 10-200 MHz)
Diffrazione di Bragg modulata
Uscita: portante modulata in frequenza

Modulatore elettro-ottico (EOM):
Idem ,ma onda generata da campo elettrico oscillante

Mode-locking si ottiene (in genere) introducendo sidebands nei modi ottici della cavità
Queste sidebands sono modulate (AM o FM) in fase tra loro

LASER fs REALISTICI

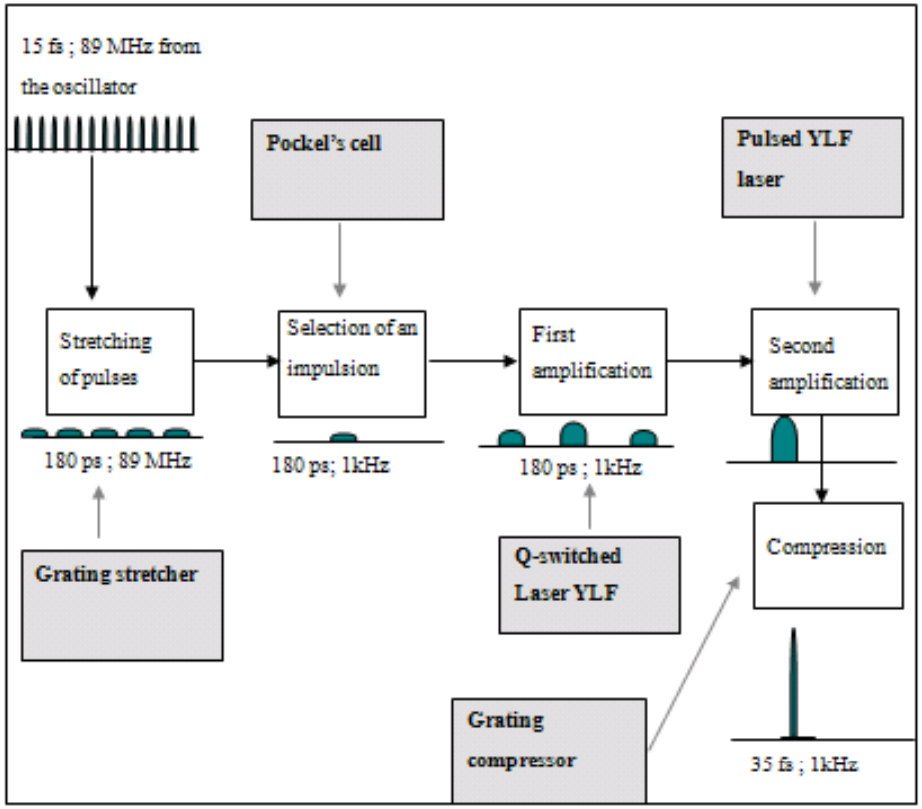

In genere l'oscillatore è seguito da stadi di amplificazione (per emissione stimolata)

Per aumentare l'efficienza di amplificazione (con pompaggio ottico da altri laser) generalmente gli impulsi si allungano e poi si ricomprimono

Il controllo della durata dell'impulso si fa con ottica dispersiva

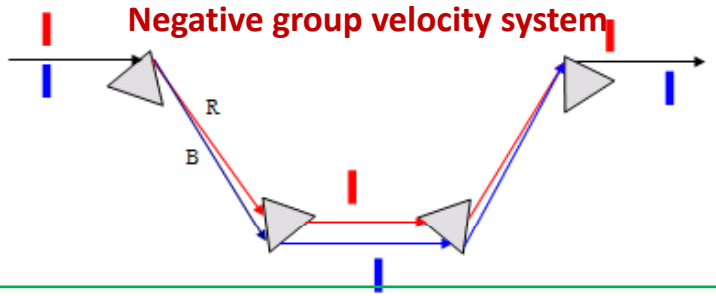

Performance tipica:
- Impulsi da decine di fs
- Frequenze di ripetizione ~ kHz - MHz
- Energia impulso ~ 1 – 10 mJ
- Lunghezza d'onda ~ 700 – 800 nm

Uso prevalente:
- spettroscopia di sistemi molecolari (eccitazione diretta della dinamica molecolare)
- trattamento materiali (per evitare formazione di plasma)

Nota: per t ~ fs principio di indeterminazione stabilisce $\Delta\nu \sim \nu$
Sorgenti (coerenti?) di luce bianca…

MODE-LOCKING PASSIVO IN FIBRA

1.5-µm Femtosecond Erbium Fiber Lasers

Erbium-doped fibers, as otherwise used mainly for erbium-doped fiber amplifiers, exhibit a broad gain bandwidth, with a maximum either at 1535 nm or at some longer wavelength such as 1550 nm – depending on the composition of the fiber core and on the inversion level, which itself is determined by fiber length, doping concentration and resonator losses.

A particularly simple type of erbium-doped fiber laser [4] is shown in Figure 1. The linear laser resonator is terminated by a semiconductor saturable absorber mirror (SESAM) as a passive mode locker on the left-hand side and a bare fiber end (with roughly 4% Fresnel reflection) on the right-hand side. The erbium-doped fiber is pumped with a low-power laser diode, the output of which is introduced into the resonator with a dichroic fiber coupler. The fiber length determines the pulse repetition rate, and the pulse duration of e.g. some hundred femtoseconds is determined by the interplay of dispersion, nonlinearity and the gain.

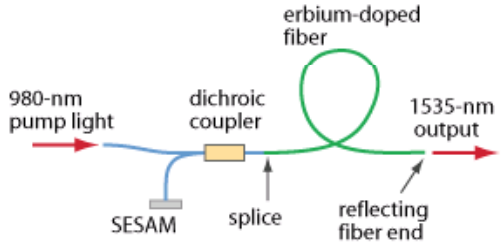

Figure 1: Simple erbium-doped femtosecond fiber laser.

Shorter pulses can be obtained from more sophisticated resonators. An example is the "figure-of-eight" laser setup [3] as shown in Figure 2. The ring on the right-hand side is a nonlinear amplifying loop mirror. Light coming from the main resonator (the left ring) is split into two counterpropagating components in the loop mirror. As the light propagating in clock-wise direction first passes a long nonlinear fiber with low power and is then amplified in the erbium-doped fiber, whereas light propagating in the other direction is amplified first, the nonlinear phase shift is larger for the latter component. If the difference in nonlinear phase shifts is π (the ideal case), the two components will interfere in such a way at the coupler in the middle that all the light is sent towards the bottom of the main resonator; light sent in the other direction will be eliminated by the isolator. The round-trip gain is thus very small for low powers, but much larger in a certain range of powers (ideally arranged to be near the peak power of the pulses). Effectively this setup acts like the combination of some laser gain with a saturable absorber, favoring the peak of a circulating pulse against the low-power background light. This artificial saturable absorber generates a single pulse circulating in the resonator and thus a pulse train emitted at the lower left port.

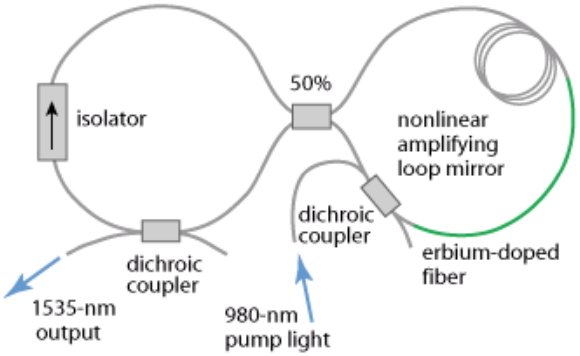

Figure 2: Figure-of-eight laser setup, with a main resonator on the left-hand side an a nonlinear amplifying loop mirror as the mode-locking element.

Fiber gratings

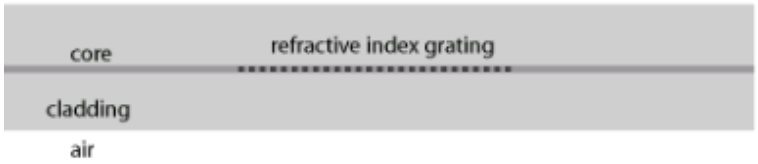

Figure 1: Schematic structure of a fiber Bragg grating (FBG). The fiber core has a periodically varying refractive index over some length. The drawing is not to scale; typical dimensions are 125µm cladding diameter and 8µm core diameter; periods of the refractive index gratings vary in the range of hundreds of nanometers or (for long-period gratings) hundreds of micrometers.

e refractive index perturbation leads to the reflection of light (propagating along the fiber) in a narrow range of wavelengths, for which a *Bragg condition* is satisfied (→ *Bragg mirrors*):

$$\frac{2\pi}{\Lambda} = 2 \cdot \frac{2\pi n_{\text{eff}}}{\lambda} \quad \Rightarrow \quad \lambda = 2 n_{\text{eff}} \Lambda$$

where Λ is the grating period, λ is the vacuum wavelength, and n_{eff} is the effective refractive index of light in the fiber.

Sistemi miniaturizzati basati su fibra

Mode-locking tramite battimento fra diverse cavità (anelli di fibra)

Produzione impulsi ultrabrevi per TLC

CONCLUSIONI

Le proprietà della luce laser sono ben interpretate sulla base del comportamento di:

- emissione stimolata
- guadagno del mezzo attivo (pompato)
- cavità ottica risonante

Esistono tecniche in grado di migliorare alcune caratteristiche della luce, in particolare quelle di larghezza di riga (monocromaticità) e quindi lunghezza di coerenza

Tecniche si Q-switching possono produrre **impulsi** laser di alta o altissima intensità, utili in numerose applicazioni (industriali e fondamentali)

Tecniche di mode-locking possono produrre impulsi **ultra-brevi** , utili in molti metodi di analisi (e anche per applicazione, ad esempio TLC)

FONTI

O. Svelto and P. Hanna, Principles of Lasers (Plenum Press, 1998)
http://www.wikipedia.org
R. Pratesi, *Dispense di Fisica dei Laser*, Università di Firenze ed INO, (http://www.ino.it/home/pratesi/DispenseL&A.htm).
W. Demtroeder, Laser Spectroscopy, (Springer, 1991)